PROCEEDINGS OF THE YEREVAN STATE UNIVERSITY

Physical and Mathematical Sciences 2023, **57**(3)

Mechanics

NUMERICAL RESULTS AND ITS ANALYSIS

A. V. KEROBYAN [1*], K. P. SAHAKYAN [2**]

[1] *Chair of Mechanics, YSU, Armenia*
[2] *Chair of General Mathematics, YSU, Armenia*

Numerical results to solving of the system of integral Eqs. (24), (27) and the integral equation (29) and its analysis.

For some cases considered problem presented above, i.e. for the systems of Fredholm integral equations (24), (27) and for the integral equation (29), the numerical results and its analysis are presented. Now, since $\alpha_1 = a_1/a,\ \beta_1 = b_1/a$ $\alpha_2 = a_2/a,\ \beta_2 = b_2/a$, and $\xi_1 = c_1/a,\ \eta_1 = d_1/a$, and accepting $a_1 = -a,\ b_1 = a,\quad a_2 = 2a,\ b_2 = 4a$, $c_1 = -a,\ d_1 = a$, we will obtain $\alpha_1 = -1,\ \beta_1 = 1,\quad \alpha_2 = 2,\ \beta_2 = 4$, and $\xi_1 = -1,\ \eta_1 = 1$. Further, it is accepted that $\delta_1^2 = \overline{\delta}_1^2 = \delta^*$, (in this case we have $b_3^* = b_1^*$). Then the system of integral equations (24) we will represent in the following form:

$$p_1^*(x) = \delta^* \int_{-1}^{1} M_1^*(x,t)\, p_1^*(t)\, dt + \delta^* \theta \int_{2}^{4} M_1^*(x,t)\, p_2^*(t)\, dt + \delta^* \theta_1 \int_{-1}^{1} H_1^*(x,\tau)\, q_1^*(\tau)\, d\tau + f(x),$$
$$-1 \le x \le 1, \qquad (24\text{a})$$

$$p_2^*(x) = \delta^* \int_{2}^{4} M_2^*(x,t)\, p_2^*(t)\, dt + \delta^* \theta^{-1} \int_{-1}^{1} M_2^*(x,t)\, p_1^*(t)\, dt + \delta^* \theta_2 \int_{-1}^{1} H_2^*(x,\tau)\, q_1^*(\tau)\, d\tau + g(x),$$
$$2 \le x \le 4,$$

$$q_1^*(x) = \delta^* \int_{-1}^{1} R^*(x,\tau)\, q_1^*(\tau)\, d\tau + \delta^* \theta_1^{-1} \int_{-1}^{1} T^*(x,\tau)\, p_1^*(t)\, dt + \delta^* \theta_2^{-1} \int_{2}^{4} T^*(x,t)\, p_2^*(t)\, dt + q(x),$$
$$-1 \le x \le 1.$$

Then the system of integral Eq. (27) will be written in the form:

$$p_1^*(x) = \delta^* \int_{-1}^{1} M_1^*(x,t)\, p_1^*(t)\, dt + \delta^* \theta_1 \int_{-1}^{1} H_1^*(x,\tau)\, q_1^*(\tau)\, d\tau + f(x), \quad -1 \le x \le 1, \qquad (27\text{a})$$

* E-mail: agas50@ysu.am
** E-mail: karen_sahakyan@ysu.am

$$q_1^*(x)=\delta^*\int_{-1}^{1}R^*(x,\tau)q_1^*(\tau)d\tau+\delta^*\theta_1^{-1}\int_{-1}^{1}T^*(x,t)p_1^*(t)dt+q(x),\quad -1\le x\le 1,$$

and the integral equation (29) in the form:

$$p_1^*(x)=\delta^*\int_{-1}^{1}M_1^*(x,t)p_1^*(t)dt+f(x),\quad -1\le x\le 1. \tag{29a}$$

Here the following notations are introduced:

$p_j^*(x)=\varphi_j(x)/P_j,\ j=1,2,\ q_1^*(x)=\psi(x)/Q,\ \ \theta=P_2/P_1,\theta_1=Q/P_1,$

$\theta_2=Q/P_2,\ h_k^*=h_k/a,\ h_j^*=h_j/a,\ h_i^*=h_i/a,\ \kappa_j=E_j/E,\ j=1,2,$

$\kappa_i=E_i/E,i=3,$

$$f(x)=\frac{\gamma_1^*\cos h\left[\gamma_1^*(x+1)\right]}{\sin h\left(2\gamma_1^*\right)},\ g(x)=\frac{\gamma_2^*\cos h\left[\gamma_2^*(x-2)\right]}{\sin h\left(2\gamma_2^*\right)},$$

$$q(x)=\frac{\alpha^*\cos h\left[\alpha^*(x+1)\right]}{\sin h\left(2\alpha^*\right)},$$

$$\gamma_j^*=a\gamma_j=\left(\frac{\kappa_j E h_k^* h_j^*}{G_k}\right)^{-\frac{1}{2}},\ j=1,2,\qquad \alpha^*=a\alpha=\left(\frac{\kappa_i E h_k^* h_i^*}{G_k}\right)^{-\frac{1}{2}},$$

$$M_1^*(x,t)=\ln|x-t|-\gamma_1^*\int_{-1}^{1}G_1^*(x,s)\ln|s-t|ds,\ \ M_1^*(x,t)=-M_1(x,t)\ ,$$

$$M_2^*(x,t)=\ln|x-t|-\gamma_2^*\int_{2}^{4}G_2^*(x,s)\ln|s-t|ds,\quad M_2^*(x,t)=-M_2(x,t),$$

$$R^*(x,\tau)=\ln|x-\tau|-\alpha^*\int_{-1}^{1}K^*(x,v)\ln|v-\tau|dv,\ R^*(x,\tau)=-R(x,\tau),$$

$$H_1^*(x,\tau)=\frac{1}{2}\left\{\ln\left[(x-\tau)^2+l_*^2\right]+\frac{2\kappa l_*^2}{\left[(x-\tau)^2+l_*^2\right]}\right\}-$$

$$-\frac{\gamma_1^*}{2}\int_{-1}^{1}G_1^*(x,s)\left\{\ln\left[(s-\tau)^2+l_*^2\right]+\frac{2\kappa l_*^2}{\left[(s-\tau)^2+l_*^2\right]}\right\}ds,$$

$$H_2^*(x,\tau)=\frac{1}{2}\left\{\ln\left[(x-\tau)^2+l_*^2\right]+\frac{2\kappa l_*^2}{\left[(x-\tau)^2+l_*^2\right]}\right\}-$$

$$-\frac{\gamma_2^*}{2}\int_{2}^{4}G_2^*(x,s)\left\{\ln\left[(s-\tau)^2+l_*^2\right]+\frac{2\kappa l_*^2}{\left[(s-\tau)^2+l_*^2\right]}\right\}ds,$$

$$T^*(x,t)=\frac{1}{2}\left\{\ln\left[(x-t)^2+l_*^2\right]+\frac{2\kappa l_*^2}{\left[(x-t)^2+l_*^2\right]}\right\}-$$

$$-\frac{\alpha^*}{2}\int_{-1}^{1}K^*(x,v)\left\{\ln\left[(v-t)^2+l_*^2\right]+\frac{2\kappa l_*^2}{\left[(v-t)^2+l_*^2\right]}\right\}dv,$$

$$H_1^*(x,\tau)=-H_1(x,\tau),\ H_2^*(x,\tau)=-H_2(x,\tau),\ T^*(x,t)=-T(x,t),$$

$$G_1^*(x,s)=\frac{1}{\sin h(2\gamma_1^*)}\begin{cases}\cos h\left[\gamma_1^*(x-1)\right]\cos h\left[\gamma_1^*(s+1)\right], & x>s,\\ \cos h\left[\gamma_1^*(x+1)\right]\cos h\left[\gamma_1^*(s-1)\right], & x<s,\end{cases}$$

$$G_2^*(x,s)=\frac{1}{\sin h(2\gamma_2^*)}\begin{cases}\cos h\left[\gamma_2^*(x-4)\right]\cos h\left[\gamma_2^*(s-2)\right], & x>s,\\ \cos h\left[\gamma_2^*(x-2)\right]\cos h\left[\gamma_2^*(s-4)\right], & x<s.\end{cases}$$

$$K^*(x,v)=\frac{1}{\sin h(2\alpha^*)}\begin{cases}\cos h\left[\alpha^*(x-1)\right]\cos h\left[\alpha^*(v+1)\right], & x>v,\\ \cos h\left[\alpha^*(x+1)\right]\cos h\left[\alpha^*(v-1)\right], & x<v,\end{cases}$$

Further, after calculations of respective integrals correspond to (35), (36), in considering cases when the values of corresponding parameters are : a) $l_*=1$ and $\kappa=0.5$ (in this case for the Poisson ratio ν acceptable values are 0.3 to 0.35), for the system of integral equations (24a) according to (37), we obtain the condition of solvability by the method of successive approximations in the form $\delta^*<0.135$ (in this case, we obtain $c_{11}=c_{22}=c_{33}\approx 2.76$, $c_{12}=c_{21}\approx 2.20$, and $c_{13}=c_{31}\approx 1.34$, $c_{23}=c_{32}\approx 2.44$). When the values of corresponding parameters are : b) $l_*=1.5$ and $\kappa=0.5$, we obtain the condition of solvability in the form $\delta^*<0.131$ (in this case, we obtain $c_{11}=c_{22}=c_{33}\approx 2.76$, $c_{12}=c_{21}\approx 2.20$, and $c_{13}=c_{31}\approx 1.90$, $c_{23}=c_{32}\approx 2.66$).

For the system of integral equations (27a) when the values of corresponding parameters are: a) $l_*=1$ and $\kappa=0.5$, according to (38) we obtain the condition of solvability by the method of successive approximations in the form $\delta^*<0.244$ (in this case we obtain $c_{11}^*=c_{22}^*\approx 2.76$, $c_{12}^*=c_{21}^*\approx 1.34$), and when the values of corresponding parameters are: b) $l_*=1.5$ and $\kappa=0.5$, we obtain the condition of solvability in the form $\delta^*<0.214$ (in this case we obtain $c_{11}^*=c_{22}^*\approx 2.76$, $c_{12}^*=c_{21}^*\approx 1.90$), where corresponding to the above now the following notations are introduced: $c_{11}^*=c_{11}$, $c_{22}^*=c_{33}$, and $c_{12}^*=c_{13}$, $c_{21}^*=c_{31}$, respectively.

For the integral equation (29a) according to (39) we obtain the condition of solvability by the method of successive approximations in the form $\delta^*<0.36$.

The numerical results solving of the systems of integral equations (24a), (27a) and of the integral equation (29a), by the method of successive approximations for various values of characteristic parameters δ^*, $\gamma_j^*\left(j=1,2\right)$ and α^*, respectively, when $\theta=1$, $\theta_1=1$, $\theta_2=1$ are obtained in the form of tables and graphics. The calculations have been done by using "Mathematica 9.0" program.

In calculations for the material of the adhesive layers are selected the adhesive Redux 775 [1] with the Young's modulus $E_k=3.35\,GPa$, or the shear modulus $G_\kappa=1.20\,GPa$, and Poisson's ratio $\nu_\kappa=0.395$ (used in aircraft structures for bonded metal to metal and other construction materials, particularly to affix stiffening stringers [1]).

For the adhesive thickness h_k^* (for all types of adhesive Redux) practically acceptable values are 0.004 to 0.01 inches (or 0.1 to 0.25 *mm*) [1]), everywhere in the calculations it is accepted $h_k^*=2.5\cdot10^{-2}$ (unit, in *cm*), and for the thickness of stringers are accepted $h_j^*=40h_k^*$, and $h_i^*=40h_k^*$. Then accepting for the ratio $E/G_k=10^2$, which is realized when $E=120\,GPa$ (f. ex., bronze [2]), and $h/b_1^*=0.4$, in the cases $\kappa_j=3\ \left(j=1,2\right)$, and $\kappa_i=3\left(i=3\right)$, we obtain $\gamma_j^*=0.35$, and $\alpha^*=0.35$ (here and below index j is accepts the values $j=1,2$ and index i is accept the value $i=3$), in the cases $\kappa_j=2.5$ and $\kappa_i=2.5$, we obtain $\gamma_j^*=0.4$ and $\alpha^*=0.4$, in the cases $\kappa_j=1.6$ and $\kappa_i=1.6$, we obtain $\gamma_j^*=0.5$ and $\alpha^*=0.5$ (its corresponds to the materials of steel [2]), in the cases $\kappa_j=1$ (i.e. when $E_j=E$) and $\kappa_i=1$, we obtain $\gamma_j^*=0.6$ and $\alpha^*=0.6$ (its corresponds to the materials of bronze [2]). In considering cases for the parameter δ^* we obtain $\delta^*\approx0.28$.

Note that in the cases $\kappa_j=1$ and $\kappa_i=1$, i.e. when the materials of the sheet and stringers are aluminium alloy [2] with modulus of elasticity $E=75\,GPa$ and the Poisson ratio $\nu=0.35$ (in this case the ratio $E/G_k=0.6\cdot10^2$), we obtain $\delta^*=0.3$, $\gamma_j^*=0.85$, and $\alpha^*=0.85$. Then, when $\delta^*=0.3$ and $\gamma_j^*=0.5$, $\alpha^*=0.5$ for the modulus of elasticity of the stringers we obtain $E_j=E_i=200\,GPa$ (it is corresponds to the material of steel [2]). For the values $\delta^*=0.3$ and $\gamma_j^*=0.6$, $\alpha^*=0.6$, for E_j and E_i we obtain $E_j=E_i=140\,GPa$ and for values $\delta^*=0.3$ and $\gamma_j^*=0.7$, $\alpha^*=0.7$, for E_j we obtain $E_j=E_i=100\,GPa$ (corresponds to the materials of titanium, brass [2]).

Some numerical results solving of integral equation (29a) for various values of parameters δ^* and $\gamma_1^*=\gamma^*$, where is introduced also notation $p^*\left(x\right)=p_1^*\left(x\right)$, are presented below in the form of graphics. The curves, presented on Figs. 2 and 3, graphically illustrate corresponding solutions of Eq. (29a) obtained by the method of successive approximations (they are convergent on the sixth approximations) for various values of δ^* and γ^*. In this case, according to the condition of solvability of equation (29a), for values of the parameter $\delta^* = 0.2$ and γ^*, on Fig. 2 the curves I, II and III – correspond to values of $\delta^* = 0.2$ and $\gamma^* = 0.35$; $\gamma^* = 0.5$; $\gamma^* = 0.6$, respectively, and on Fig. 3 the curves I, II and III – correspond to values of $\delta^* = 0.3$; and $\gamma^* = 0.6$; $\gamma^* = 0.7$; $\gamma^* = 0.85$, respectively.

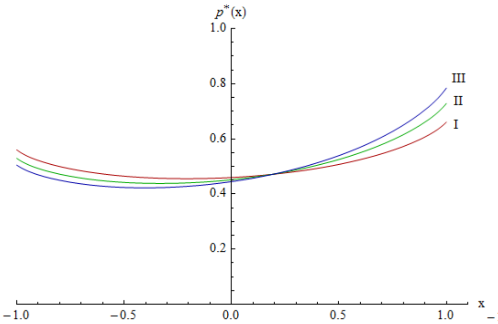

Fig. 2.

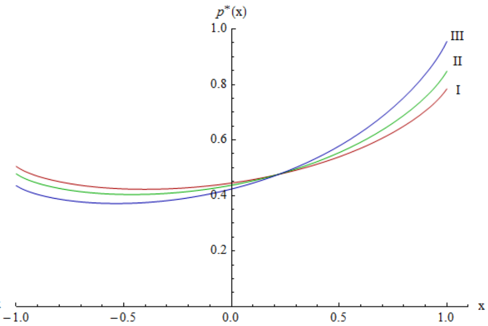

Fig. 3.

The curves I*, II* and III* presented respectively on Figs. 4 and 5, illustrate the law of distribution of unknown shear forces acting under the finite stringer in the case of the absolute rigid sheet (i.e. when $\delta^* = 0$). They are simultaneously correspond and the starting solutions (or the zero approximations) of integral equation (29a) in form of curves, for various values of γ^*, i.e. on Fig. 4 the curves I*, II* and III* – correspond to the values of parameters $\delta^* = 0$ and $\gamma^* = 0.35$; $\gamma^* = 0.5$; $\gamma^* = 0.6$ respectively, and on Fig. 5 the curves I*, II* and III* – correspond to the values of parameters $\delta^* = 0$ and $\gamma^* = 0.6$; $\gamma^* = 0.7$; $\gamma^* = 0.85$ respectively.

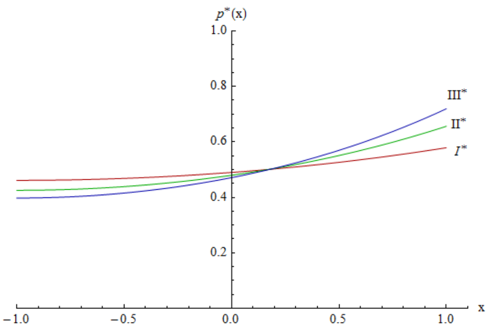

Fig. 4.

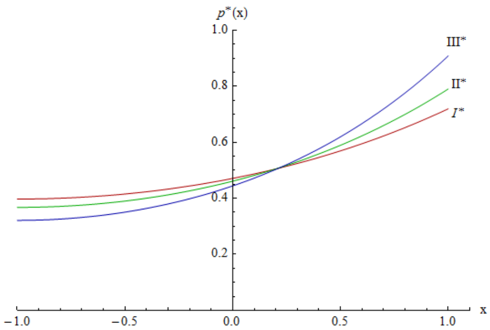

Fig. 5.

From the calculations and corresponding graphics it follows that, with decrease in the values of the parameter γ^* shear forces decrease near the end point of stringer $x=1$, and to the contrary increase near the end point of stringer $x=-1$. It means, the more rigid the material of stringer is the more symmetrical unknown shear forces are distributed under the stringer with respect to the middle part of the finite stringer, otherwise shear forces are concentrated near the end point of stringer where the force is acting. Then, by a decrease in the values of the parameter δ^* with the same values of γ^* corresponding values of shear forces are decreased.

On Fig. 6 the curves I, II and III show the law of distribution of unknown shear forces in the case of rigid stringer, i.e. when $\gamma^* \to 0$ (in the calculations it is accepted $\gamma^* = 1 \cdot 10^{-6}$). Here the curve I – correspond to values of parameters $\delta^* = 0$ and $\gamma^* \approx 0$, i.e. when the materials of both the sheet and the stringer become rigid. In this case shear forces are distributed evenly and obtained the same constant value $p^*(x) = 0.5$. The curves II and III presented on Fig. 6 correspond to values of parameters $\gamma^* \approx 0$ and $\delta^* = 0.2$, $\delta^* = 0.3$, respectively, in which shear forces are distributed symmetrically with respect to the middle part of the finite stringer.

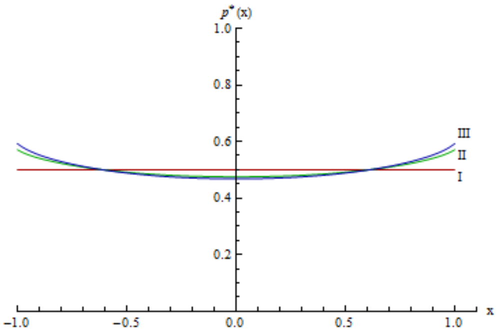

Fig. 6.

Note that, changing the length of the finite stringer, will be changed and the condition of solvability of corresponding to integral equation (29a), as well as their corresponding the law of distribution of unknown shear forces. In case when the length of stringer grow one and half times, for example, when the stringer will be on the segment [1, 4], according to (39) we obtain the condition of solvability of corresponding to equation (29a) in the form $\delta^* < 0.28$ (in this case we obtain $c_1^{'} = c_{11}^* \approx 3.56$).

In case when the length of stringer grow twice, i.e. when the stringer located on the segment [1, 5], we obtain the condition of solvability of corresponding to equation (29a) in the form $\delta^* < 0.22$ (in this case we obtain $c_1^{''} = c_{11}^* \approx 4.5$).

For the same values of parameters δ^* and γ^* presented above, on Fig. 2, in the considered cases the law of distribution of shear forces are presented below on Figs. 7.1 and 8.1, respectively. On Figs. 7.1 and 8.1, the curves I, II and III –

correspond to values of parameters $\delta^* = 0.2$ and $\gamma^* = 0.35$; $\gamma^* = 0.5$; $\gamma^* = 0.6$, respectively, and on Figs. 7.2 and 8.2 the curves I*, II* and III*– correspond to the values of parameters $\delta^* = 0$ and $\gamma^* = 0.35$; $\gamma^* = 0.5$; $\gamma^* = 0.6$ respectively.

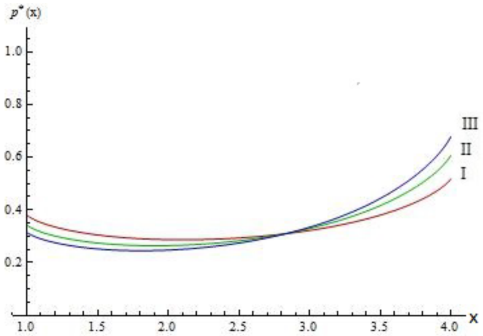

Fig. 7.1

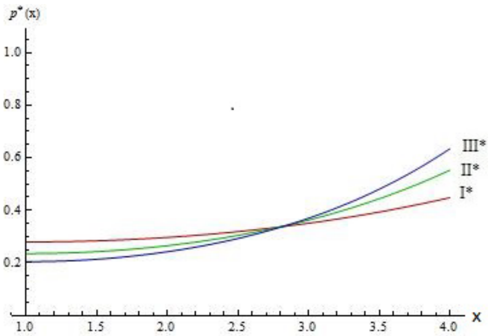

Fig. 7.2

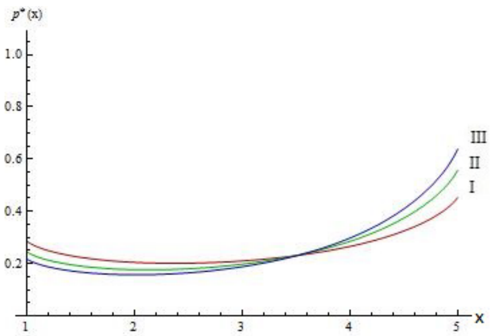

Fig. 8.1.

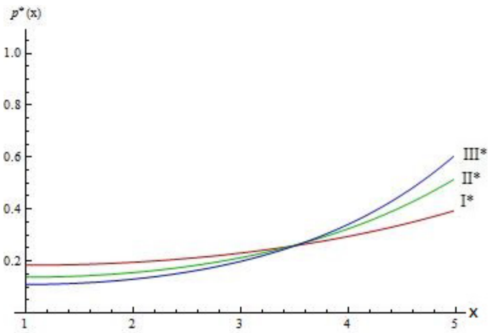

Fig. 8.2.

Comparing the results of calculations which graphically are presented on Figs. 2, 7.1 and 8.1, respectively, it is shown that, growing the length of stringer in the considered cases the corresponding values of shear forces in the same points respectively, are decreased significantly.

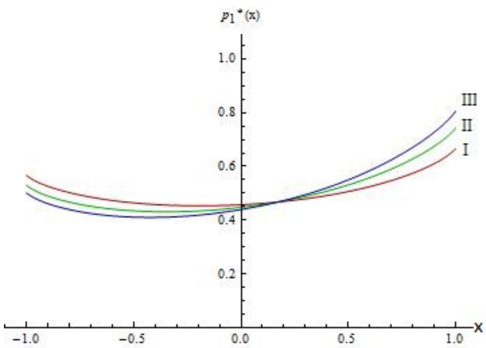

Fig. 9.1.

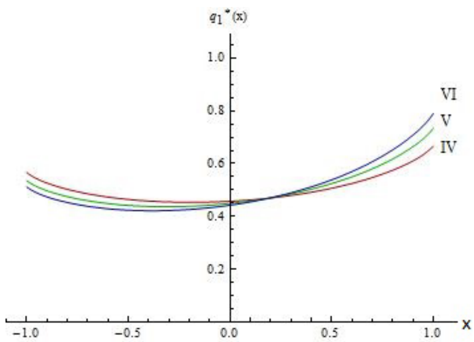

Fig. 9.2.

Some numerical results solving of the system of integral equations (27a) for various values of parameters δ^* and γ_1^*, α^*, when $l_* = 1$ are presented below in the form of graphics. The curves presented on Figs. 9.1 and 9.2 graphically illustrate the corresponding solutions of the system (27a) obtained by the method of successive approximations for various values of δ^* and γ_1^*, α^*, respectively. In this case, according to the condition of solvability of the system (27a), as shown above, for values of the parameter $\delta^* = 0.2$, on Figs. 9.1 and 9.2, the curves I and IV – correspond also to the values of parameters $\gamma_1^* = \alpha^* = 0.35$, respectively, the curves II and V – correspond to values of parameters $\gamma_1^* = \alpha^* = 0.5$, respectively, the curves III and VI correspond to values of parameters $\gamma_1^* = \alpha^* = 0.6$, respectively. The curves, presented on Figs. 10.1 and 10.2, respectively, represented the law of distribution of unknown shear forces acting under two parallel finite stringers in the case of rigid sheet (i.e. when $\delta^* = 0$). They are simultaneously correspond also starting solutions (or the zero approximations) of the system of integral equations (27a) obtained by the method of successive approximations for values of parameters γ_1^* and α^*, respectively, in the form of curves I*, II*, III* and IV*, V*, VI*, respectively.

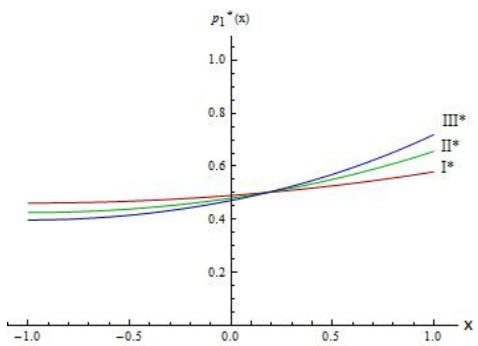

Fig. 10.1.

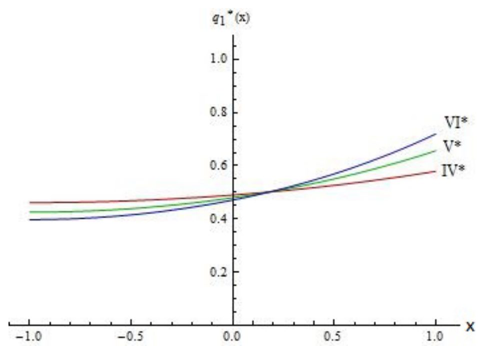

Fig. 10.2.

On Figs. 10.1 and 10.2, the curves I* and IV* – correspond to values of $\delta^* = 0$ and $\gamma_1^* = \alpha^* = 0.35$, respectively, the curves II* and V* – correspond to values of $\gamma_1^* = \alpha^* = 0.5$, respectively, and the curves III* and VI* – correspond to values of $\gamma_1^* = \alpha^* = 0.6$, respectively.

From the calculations and corresponding graphics presented on Figs. 9.1 and 9.2, it follows that, on these segments, in the considered case we have exactly the same law of distribution of shear forces (i.e. in the same points corresponding values of shear stresses are exactly the same). Comparing the results of calculations which graphically are presented on Figs. 9.1 and 2, respectively, it is shown that, in the considered case the corresponding values of shear forces in the same points respectively, are increased by values 0.02.

Note that, in the case when $l_* = 1.5$, for the same values of the parameters $\delta^* = 0.2$ and γ_1^*, α^*, respectively, presented above, we will have such a distributions of shear forces as they are presented on Figs. 9.1, 9.2 (in this case the corresponding values of shear forces a little are decreased (by values 0.05)).

Further, changing the horizontal distance between two parallel finite stringers, leaving their length the same, the law of distribution of shear forces will be changed. In case when two parallel stringers are arranged on the segments [–1, 1] and [1, 3], respectively, we will obtain the condition of solvability of corresponding to (27a) system in the form $\delta^* < 0.21$ (in this case $c_{11}^* = c_{22}^* \approx 2.76$, $c_{12}^* = c_{21}^* \approx 2.0$). In this case for the same values of the parameters $\delta^* = 0.2$, and γ_1^*, α^* on Figs. 11 .1, and 11.2, the curves I and IV – correspond to values of parameters $\gamma_1^* = \alpha^* = 0.35$, respectively, the curves II and V – correspond to values of parameters $\gamma_1^* = \alpha^* = 0.5$, respectively, the curves III and VI – correspond to values of parameters $\gamma_1^* = \alpha^* = 0.6$, respectively. Note that, for the stringer which arranged on the segment [1, 3], near the end point of the stringer $x = 3$ the correspond values of shear forces are increased and to the contrary are decreased near the end point of the stringer $x = 1$.

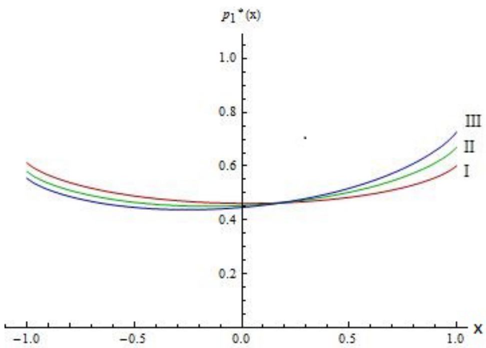

Fig. 11.1.

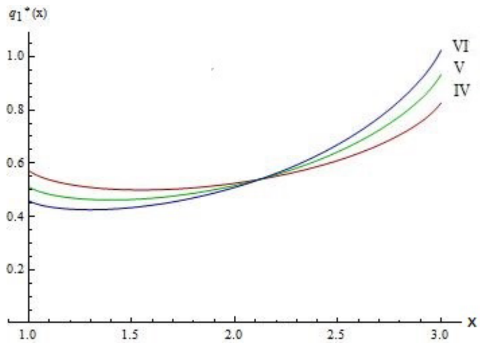

Fig. 11.2.

In case when two parallel stringers arranged on the segments [–1, 1] and [2, 4], respectively, we will obtain the condition of solvability of corresponding to (27a) system in the form $\delta^* < 0.205$. For the same values of the parameters $\delta^* = 0.2$, and γ_1^*, α^* respectively, on Figs. 12.1, and 12.2, the curves I and IV – correspond to values of parameters $\gamma_1^* = \alpha^* = 0.35$, respectively, the curves II and V – correspond to values of parameters $\gamma_1^* = \alpha^* = 0.5$, respectively, the curves III and VI – correspond to values of parameters $\gamma_1^* = \alpha^* = 0.6$, respectively. Note that, in the considered case for the stringer which is arranged on the segment [2, 4] near the end point of the stringer $x = 2$ and $x = 4$, corresponding values of shear forces are increased.

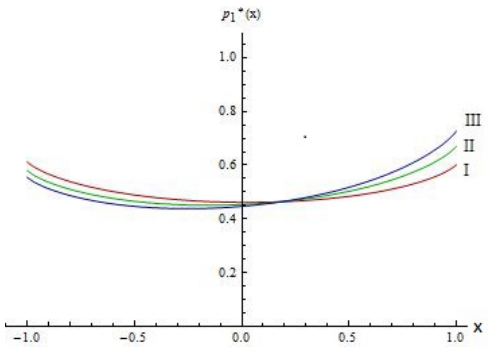

Fig. 12.1.

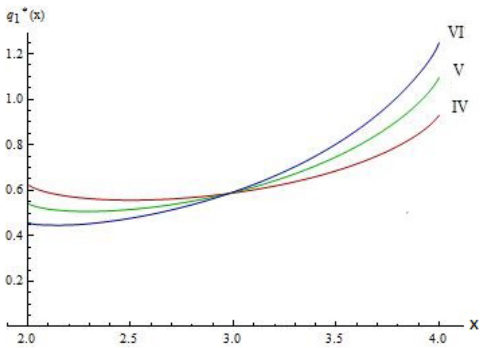

Fig. 12.2.

Now to the contrary, when two parallel stringers are arranged on the segments [1, 3] and [−1, 1], respectively, for the same values of the parameters $\delta^* = 0.2,$ and γ_1^*, α^* respectively, the law of distribution of shear forces are presented below on Figs. 13.1 and 13.2, respectively.

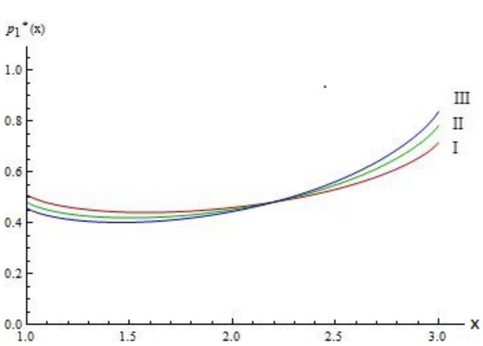

Fig.13.1.

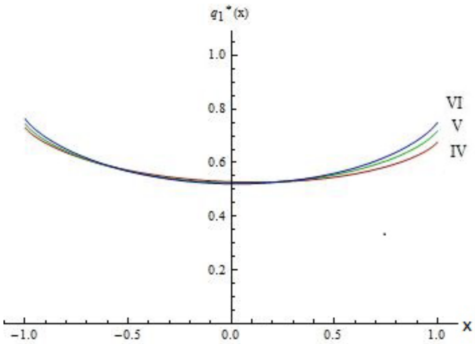

Fig.13.2.

In case when two parallel stringers are arranged on the segments [2, 4] and [−1, 1], respectively, for the same values of the parameters $\delta^* = 0.2,$ and γ_1^*, α^* respectively, the law of distribution of shear forces are presented below on Figs. 14.1 and 14.2.

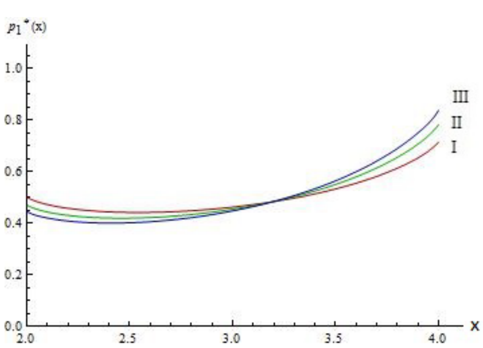

Fig. 14.1.

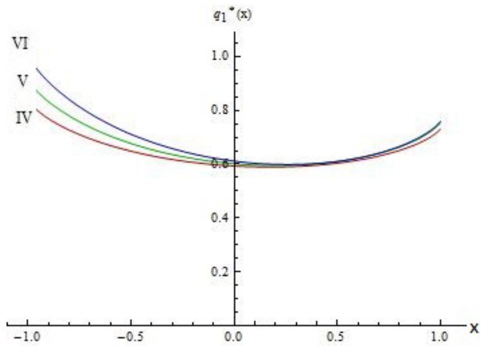

Fig. 14.2.

From these calculations and corresponding graphics presented on Figs. 13.1 and 13.2, and on Figs. 14.1 and 14.2, respectively, it follows that, in the considered cases for the stringer which arranged on the segment [–1, 1] near the end point of the stringer $x=1$ (i.e. near the end point of stringer where the concentrated force is applied) the corresponding values of shear forces are decreased and to the contrary near the end point of stringer $x=-1$ are increased. In the considered cases on all segments for the starting solutions we will have such distributions of shear forces as they are presented on Figs. 10.1, and 10.2, respectively.

Some numerical results solving the system of integral equations (24a) for various values of parameters δ^* and γ_1^*, γ_2^* and α^* when $l_*=1$ are presented below in the form of graphics. The curves presented on Figs. 15.1, 15.2 and 15.3 graphically illustrate the corresponding solutions of the system (24a) obtained by the method of successive approximations for various values of δ^* and γ_1^*, γ_2^* and α^*.

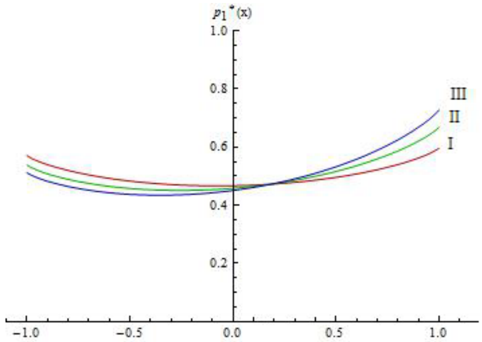

Fig. 15.1.

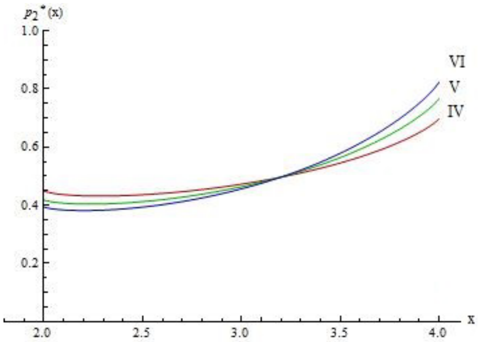

Fig.15.2.

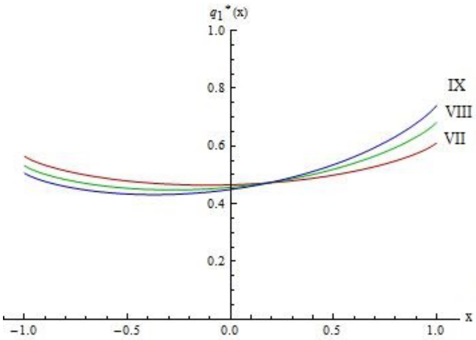

Fig. 15.3.

In case for value of parameter $\delta^*=0.13$ (since already we have obtained the condition of solvability of the system (24a) in the form $\delta^*<0.135$) on Figs. 15.1, 15.2 and 15.3 the curves I, IV and VII – correspond to values of parameters $\gamma_1^*=\gamma_2^*=\alpha^*=0.35$, respectively, the curves II, V and VIII – correspond to values of parameters $\gamma_1^*=\gamma_2^*=\alpha^*=0.5$, respectively, the curves III, VI and IX – correspond to values of parameters $\gamma_1^*=\gamma_2^*=\alpha^*=0.6$, respectively. Further, according to corresponding calculations it follows that, the curves I, V and VII –

presented on Figs. 15.1, 15.2 and 15.3 by a little mistake also correspond to values of $\delta^* = 0.13$ and $\gamma_2^* = 0.35$, $\gamma_2^* = 0.5$ and $\alpha^* = 0.35$ respectively, the curves I, VI, VIII – correspond to values of $\gamma_1^* = 0.35$; $\gamma_2^* = 0.6$ and $\alpha^* = 0.5$, respectively, etc.

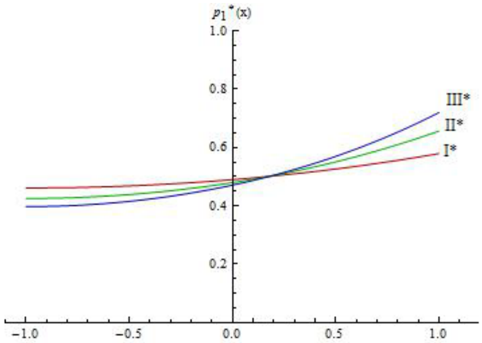

Fig. 16.1.

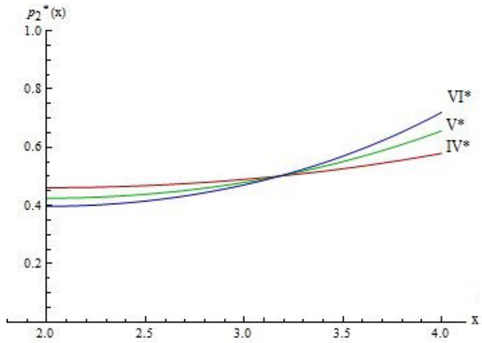

Fig. 16.2.

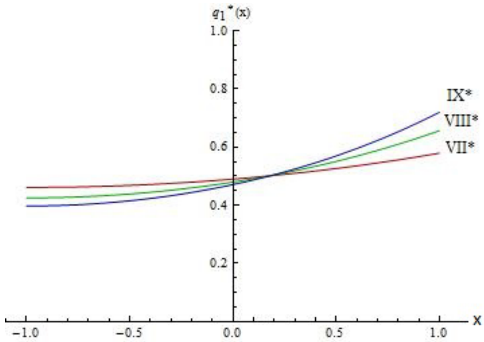

Fig. 16.3.

The curves, presented on Figs. 16.1, 16.2 and 16.3, respectively, represent the law of distribution of shear forces acting under three finite stringers in the case of rigid sheet. They are simultaneously correspond also to the starting solutions of the system of integral equations (24a) obtained by the method of successive approximations for various values of parameters γ_1^*, γ_2^* and α^* in the form of curves I*, II* , III* , IV*, V*, VI* and VII*, VIII*, IX*, correspondingly. On Figs. 16.1, 16.2 and 16.3 the curves I*, IV* and VII* – correspond to values of $\delta^* = 0$ and $\gamma_1^* = \gamma_2^* = \alpha^* = 0.35$, respectively, the curves II*, V* and VIII* – correspond to values of $\gamma_1^* = \gamma_2^* = \alpha^* = 0.5$, respectively, and the curves III*, VI* and IX* – correspond to values of $\gamma_1^* = \gamma_2^* = \alpha^* = 0.6$, respectively. The curves I*, V* and IX* – correspond to values of $\gamma_1^* = 0.35$; $\gamma_2^* = 0.5$ and $\alpha^* = 0.6$, respectively, etc.

In case when the material of tree finite stringers two of which become rigid, the law of distribution of shear forces are presented below in the form of graphics. When the materials of both stringers which are arranged along the same line become rigid, the law distributions of shear forces are presented below in the form of graphics. On Figs. 17.1, 17.2 and 17.3 for values of parameter $\delta^* = 0.13$ the curves I, IV and VII – correspond also to values of parameters $\gamma_1^* \approx 0$; $\gamma_2^* \approx 0$ (in the calculations also they are accepted $\gamma_1^* = 1 \cdot 10^{-6}$ $\gamma_2^* = 1 \cdot 10^{-6}$) and $\alpha^* = 0.35$, respectively, the curves II, V and VIII – correspond to values of $\gamma_1^* \approx 0$; $\gamma_2^* \approx 0$ and $\alpha^* = 0.5$, respectively, the curves III , VI and IX – correspond to values of $\gamma_1^* \approx 0$; $\gamma_2^* \approx 0$ and $\alpha^* = 0.6$, respectively.

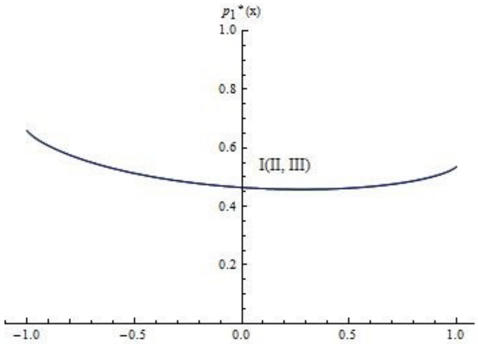

Fig. 17.1.

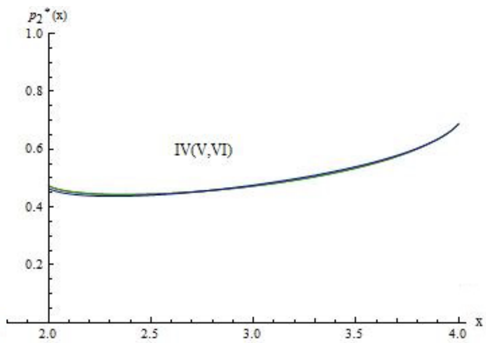

Fig. 17.2.

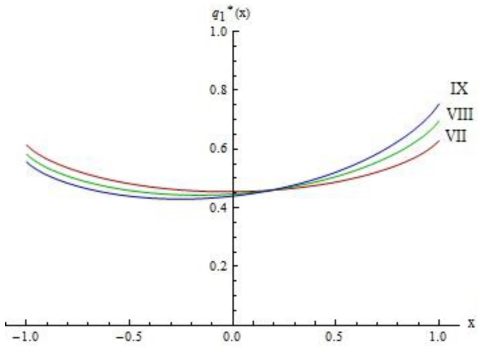

Fig. 17.3.

For the above considered cases also below graphically are presented the results of the calculations in the cases of rigid sheet. On Figs. 18.1, 18.2 and 18.3 the curves I*, IV*and VII* – correspond to values of $\delta^* = 0$ and $\gamma_1^* \approx 0,$ $\gamma_2^* \approx 0,$ and $\alpha^* = 0.35,$ respectively, the curves II*, V* and VIII* – correspond to values of $\gamma_1^* \approx 0,$ $\gamma_2^* \approx 0,$ and $\alpha^* = 0.5,$ respectively, and the curves III*, VI* and IX* – correspond to values $\gamma_1^* \approx 0,$ $\gamma_2^* \approx 0,$ and $\alpha^* = 0.6,$ respectively.

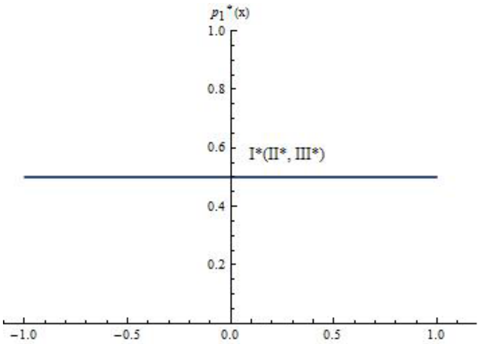

Fig.18.1.

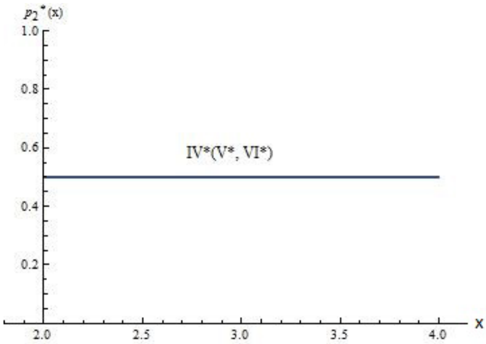

Fig.18.2.

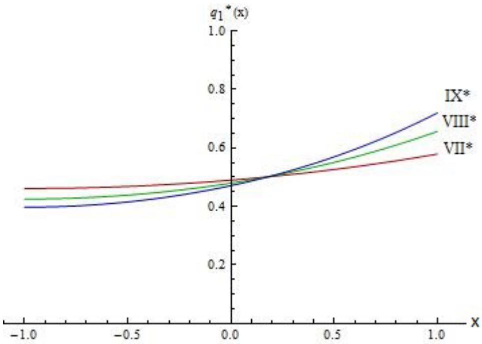

Fig. 18.3.

From these calculations and corresponding graphics it is followed, if in cases of one rigid stringer or two parallel rigid stringers, shear forces are distributed symmetrically with respect to the middle part of the stringers, so in case of three finite stringers when the materials of two finite stringers which are arranged on the same line become rigid, the symmetry is broken, which is caused by a significant impact of two neighboring stringers on each other.

In case when the materials of the sheet and three finite stringers become rigid, i.e. when $\delta^* = 0$ and $\gamma_1^* \approx 0$; $\gamma_2^* \approx 0$, and $\alpha^* \approx 0$, shear forces are distributed evenly and take the same constant values: $p_1^*(x) = 0.5$, $x \in [-1,1]$, $p_2^*(x) = 0.5$ $x \in [2,4]$ and $q_1^*(x) = 0.5$, $x \in [-1,1]$ (see also the graphics on Figs. 18.1and18.2).

Further, changing the horizontal distance between two finite stringers, as well as vertical distance between the parallel stringers leaving their length the same, the condition of solvability of corresponding to (24a) system will be changed. For example, if we make the horizontal distance between two finite stringers bigger twice (which are arranged along the same line) the stringers already will be on the segments [–1, 1] ; [3, 5] and [–1,1], respectively, and we obtain the condition of solvability of its corresponding system in the form $\delta^* < 0.126$ (in this case $c_{11} = c_{22} = c_{33} \approx 2.76$, $c_{12} = c_{21} \approx 2.76$, and $c_{13} = c_{31} \approx 1.34$, $c_{23} = c_{32} \approx 2.44$).

For calculations taking $\delta^* = 0.12$ and for parameters γ_1^*, γ_2^* and α^*, respectively, the same corresponding values, for shear forces in this case we obtain exactly the same distributions as in the previous segments, only with a little difference of their corresponding values.

In case when the horizontal distance between two stringers are decreased i.e. when the stringers will be on the segments $[-1, 1]$; $[1.1, 3.1]$ and $[-1,1]$, respectively, the results of corresponding to (24a) system's solution for the same values of parameters δ^* and γ_1^*, γ_2^* and α^* correspond to Figs. 15.1, 15.2 and 15. 3 are presented below on Figs. 19.1, 19.2 and 19.3. Here we obtain the condition of solvability of corresponding to (24a) system of integral equations in the form $\delta^* < 0.16$ (in this case $c_{11} = c_{22} = c_{33} \approx 2.76$, $c_{12} = c_{21} \approx 1.62$, and $c_{13} = c_{31} \approx 1.34$, $c_{23} = c_{32} \approx 2.05$). On Figs. 19.1, 19.2 and 19.3 for values of $\delta^* = 0.13$, the curves I, IV and VII – correspond to values of parameters $\gamma_1^* = \gamma_2^* = \alpha^* = 0.35$, respectively, the curves II, V and VIII – correspond to values of $\gamma_1^* = \gamma_2^* = \alpha^* = 0.5$, respectively, the curves III, VI and IX – correspond to values $\gamma_1^* = \gamma_2^* = \alpha^* = 0.6$, respectively.

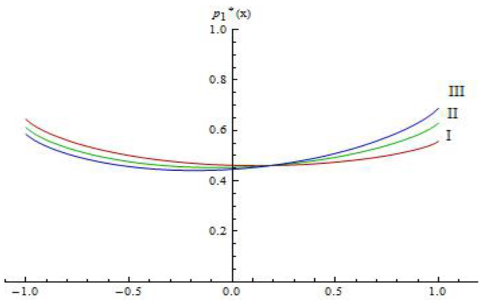

Fig. 19.1.

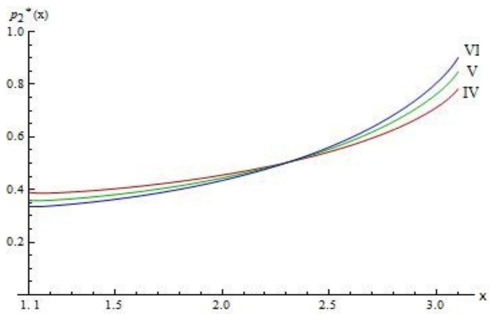

Fig. 19.2.

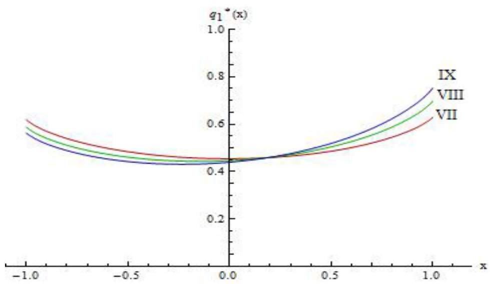

Fig. 19.3.

Comparing the results of calculations which graphically presented on Figs. 19.1, 19.2, 19.3 and Figs. 15.1, 15.2, 15.3, respectively, it is shown that, for the same values of corresponding parameters of δ^*, γ_1^*, γ_2^* and α^*, respectively, for the stringer, located on the segment $[-1, 1]$ on upper half-plane of the sheet, near the end point of stringer $x=-1$ corresponding values of shear forces $p_1^*(x)$ are increased and to the contrary are decreased near the end point of stringer $x = 1$ (i.e. near the end point of stringer where the concentrated force is applied). Then, for the stringer which is located on the segment [1.1; 3.1] corresponding values of shear forces $p_2^*(x)$ near the end point of stringer $x=1.1$ are decreased and near the end point of stringer $x=3.1$ are increased (by values 0.04). Note that, also as more rigid become the materials of the stringers, then the deference between the values of corresponding forces in the end points of stringers $x=1$ and $x=1.1$ are decreased and to the contrary, are increased on the other case. Note that, for the stringer which is located in the lower half-plane of the sheet on the segment [–1, 1] near the end point of the stringer $x=1$ the values of shear forces $q_1^*(x)$ are increased. Such a behavior of shear forces in the considered case is conditioned by the stronger interaction of stringers on each other. Note that, in the considered case for starting solutions on corresponding segments, we will have such distributions of shear forces as they are presented on Figs. 16.1, 16.2 and 16.3, respectively.

REFERENCES

1. Beevers A. *Forensic Studies of Adhesive Joints*. Report №9, Part-2-Bonded Aircraft Structure (1995), 62.
2. Feodosev V.I. *Strength of Materials*. Moscow, MSTY Publishers (1999), 592 (in Russian).